

**IMPROVEMENT OF SULFONATED POLYSULFONE MEMBRANES FOR
DIRECT METHANOL FUEL CELL: EFFECT OF ZEOLITE Y AND
SULFONATED GRAPHENE OXIDE**

Phuwadon Bunlengsuwan

A Thesis Submitted in Partial Fulfillment of the Requirements
for the Degree of Master of Science
The Petroleum and Petrochemical College, Chulalongkorn University
in Academic Partnership with
The University of Michigan, The University of Oklahoma,
Case Western Reserve University and Institut Francais du Pétrole
2015

F283685AX


Thesis Title: Improvement of Sulfonated Polysulfone Membranes for Direct Methanol Fuel cell: Effect of Zeolite Y and Sulfonated Graphene Oxide
By: Phuwadon Bunlengsuwan
Program: Petrochemical Technology
Thesis Advisors: Asst. Prof. Kitipat Siemanond
Prof. Anuvat Sirivat


Accepted by The Petroleum and Petrochemical College, Chulalongkorn University, in partial fulfillment of the requirements for the Degree of Master of Science.

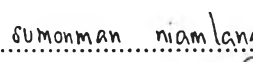

..... College Dean
(Asst. Prof. Pomthong Malakul)

Thesis Committee:


.....
(Asst. Prof. Kitipat Siemanond)


.....
(Prof. Anuvat Sirivat)


.....
(Dr. Uthaiporn Suriyaphadilok)


.....
(Dr. Sumonman Niamlang)

ABSTRACT

5671025063: Petrochemical Technology
Phuwadon Bunlengsuwan: Improvement of Sulfonated Polysulfone Membrane for Direct Methanol Fuel Cell: Effect of Zeolite Y and Sulfonated Graphene Oxide
Thesis Advisors: Asst. Prof. Dr. Kitipat Siemanond, and Prof. Anuvat Sirivat 172 pp.
Keywords: Direct methanol fuel cell/ Proton exchange membranes/ Sulfonated polysulfone/ Zeolite Y/ Sulfonated graphene oxide

The proton exchange membranes (PEMs) are being developed intensively due to their great potential as a promising power source for transportation, residential, and portable applications. In this work, the novel PEMs consisting of inorganic fillers embedded in sulfonated polysulfone (S-PSF) were fabricated. The effect of zeolite Y and sulfonated graphene oxide (S-GO) was investigated on the thermal and mechanical stability, water uptake, proton conductivity, and methanol permeability. The proton conductivity of S-PSF/zeolite Y membrane increased with increasing zeolite Y content, in parallel with the methanol permeability. It was due to its water retention property. The highest proton conductivity was found at 3 % v/v of S-GO because of the increment of sulfonic acid groups by incorporating of S-GO. The S-GO particles positively affected for blocking water and methanol molecules, caused by the increasing of interfacial interaction between S-PSF and S-GO, leading to the decreases in the water uptake and methanol permeability. Besides, the hybrid membranes, which were S-PSF membrane mixing with both zeolite Y and S-GO, were investigated. They also showed better performance than the pristine S-PSF and Nafion117 membrane. Therefore, all composite membranes are a potential candidate for being used in DMFC applications.

บทคัดย่อ

กุวคล บรรเลงสุววรรณ: การพัฒนาแผ่นเยื่อแลกเปลี่ยนโปรตอนจากซัลโฟเนท พอลิซัลโฟน เพื่อใช้ในเซลล์เชื้อเพลิงจากเมทานอล; ผลของการเติมซีโอไลต์ วายและ ซัลโฟเนท กราฟีนออกไซด์ (Improvement of Sulfonated Polysulfone Membranes for Direct Methanol Fuel Cell: Effect of zeolite Y and Sulfonated graphene Oxide) ที่ปริกษา: ผศ. ดร.กิตติพัฒน์ สีมานนท์ และ ศ.ดร. อนุวัฒน์ ศิริวัฒน์ 172 หน้า

แผ่นเยื่อแลกเปลี่ยนโปรตอน กำลังถูกพัฒนาอย่างต่อเนื่อง เพื่อเป็นแหล่งกำเนิดพลังงานแบบพกพา และประยุกต์ใช้กับยานพาหนะ และอุปกรณ์อิเล็กทรอนิกส์ แนนฟิออน (Nafion) เป็นพอลิเมอร์ที่ใช้แผ่นเยื่อแลกเปลี่ยนโปรตอนอย่างแพร่หลายในเซลล์เชื้อเพลิงจากเมทานอล เพราะมันมีความสามารถในการนำโปรตอน และคุณสมบัติทางกายภาพสูง แต่อย่างไรก็ตาม แผ่นเยื่อแลกเปลี่ยนโปรตอนจากแนนฟิออน มีจุดด้อยอยู่ที่ค่าการแพร่ผ่านของเมทานอลที่สูง ซึ่งทำให้สิ้นเปลืองเชื้อเพลิง และประสิทธิภาพของเซลล์เชื้อเพลิงนั้นลดลง อีกทั้งราคาของแผ่นเยื่อแลกเปลี่ยนโปรตอนจากแนนฟิออน นั้นค่อนข้างสูง จึงเป็นเหตุผลทำให้มีการพัฒนาแผ่นเยื่อชนิดแลกเปลี่ยนโปรตอนอย่างต่อเนื่อง ในงานวิจัยนี้ ซัลโฟเนท พอลิซัลโฟน (Sulfonated polysulfone, S-PSF) ได้ถูกเตรียมเป็นแผ่นเยื่อชนิดแลกเปลี่ยนโปรตอน โดยการเติมวัสดุเติมแต่งเข้าไป ได้แก่ซีโอไลต์ วาย (zeolite Y) และซัลโฟเนท กราฟีนออกไซด์ (Sulfonated graphene oxide, S-GO) สำหรับระบบที่เติมซีโอไลต์ วาย พบว่า ค่าการนำของโปรตอนและค่าการแพร่ผ่านของเมทานอลของแผ่นเยื่อมีค่าสูงขึ้น เนื่องจากคุณสมบัติการกักเก็บน้ำของซีโอไลต์ วาย ซึ่งสามารถช่วยให้โปรตอนเคลื่อนที่ได้ดียิ่งขึ้น และสำหรับระบบที่เติม S-GO พบว่า ค่าการนำของโปรตอนเพิ่มขึ้นได้สูงสุดที่ร้อยละ 3 โดยปริมาตร เพราะว่าสามารถเกิดอันตรกิริยาระหว่าง S-PSF และ S-GO ทำให้สามารถมีช่องว่างสำหรับเคลื่อนที่ของโปรตอนมากขึ้น แต่อันตรกิริยานี้เมื่อมีมากขึ้น จะทำให้ไปลดช่องว่างการแพร่ผ่านของน้ำและเมทานอล ส่งผลต่อการลดลงของค่าการดูดซึมของน้ำและค่าการแพร่ผ่านของเมทานอล นอกเหนือจากนี้ แผ่นเยื่อชนิดแลกเปลี่ยนโปรตอนแบบไฮบริดได้ถูกเตรียมขึ้นด้วยเช่นกัน ซึ่งแผ่นเยื่อไฮบริดนี้จะใช้ทั้งซีโอไลต์ วาย และ S-GO เป็นวัสดุเติมแต่ง โดยพบว่าแผ่นเยื่อชนิดแลกเปลี่ยนโปรตอนแบบไฮบริด ยังคงแสดงประสิทธิภาพที่ดีกว่าแผ่นเยื่อ S-PSF และ แผ่นเยื่อจากแนนฟิออน เพราะฉะนั้น จากผลการทดลองในงานวิจัยนี้แผ่นเยื่อชนิดแลกเปลี่ยนโปรตอนแบบคอมโพสิตมีศักยภาพที่ดีสำหรับการใช้ในเซลล์เชื้อเพลิงจากเมทานอล และสามารถใช้แทนจะแผ่นเยื่อจากแนนฟิออนได้อีกด้วย

ACKNOWLEDGEMENTS

I would like to take this opportunity to express my appreciation for those who have been significantly influential and responsible for my achievement in order to complete this thesis.

This research work could not be completed without the assistance and supports of following individuals and organizations.

Firstly, I would like to express my gratitude to my advisor, Asst. Prof. Kitipat Siemanond and Prof. Anuvat Sirivat who had always cared and paid attention to my research work since the beginning, giving valuable suggestions, attentive encouragement, beneficial recommendations and all the helpful supports in my research work.

Secondly, I also would like to thank to the thesis committees, Dr. Uthaiporn Suriyaphradilok and Dr. Sumonman Niamlang for their important suggestions and recommendations in my research work.

Special appreciation is given to all staff members at The Petroleum and Petrochemical College who have provided helpful assistance and many useful technical supports.

Unforgettably, appreciation is forward to all my family and friends for their cheerful encouragement, understanding, and generous supports at all time.

Finally, this research work was partially supported by the Ratchadapisek Sompoch Endowment Fund (2013), Chulalongkorn University (CU-56-900-FC), the Conductive and Electroactive Polymers Research Unit (CEAP), the Thailand Research Fund (IRG5780012), and the Royal Thai Government.

TABLE OF CONTENTS

	PAGE
Title Page	i
Abstract (in English)	iii
Abstract (in Thai)	iv
Acknowledgements	v
Table of Contents	vi
List of Tables	ix
List of Figures	x
CHAPTER	
I INTRODUCTION	1
II THEORETICAL BACKGROUND AND LITERATURE REVIEW	4
2.1 Direct Methanol Fuel Cells (DMFC)	4
2.2 Polysulfone (PSF)	12
2.3 Zeolite	24
2.4 Graphene Oxide	30
III METHODOLOGY	34
3.1 Materials and Instruments	34
3.2 Experimental Methods	35
3.2.1 Sulfonated Polysulfone and Sulfonated Graphene Oxide	35
3.2.2 Composite Membrane Preparations	35
3.3 Characterizations and Testing	36
3.3.1 Characterizations for S-PSF	36

CHAPTER	PAGE
3.3.2	37
3.3.3	37
IV	
IMPROVEMENT OF SULFONATED POLYSULFONE MEMBRANES FOR DIRECT METHANOL FUEL CELL: EFFECT OF ZEOLITE Y AND SULFONATED GRAPHENE OXIDE	40
4.1	40
4.2	41
4.3	42
4.3.1	42
4.3.2	43
4.3.3	43
4.3.4	43
4.3.5	43
4.3.6	44
4.4	46
4.4.1	46
4.4.2	47
4.4.3	48
4.4.4	53
4.5	54
4.6	54
4.7	55
V	
CONCLUSIONS	69
REFERENCES	70

CHAPTER	PAGE
APPENDICES	
Appendix A Sulfonation Process and Degree of Sulfonation	78
Appendix B Identification of FT-IR Spectrum of Polysulfone and Sulfonated Polysulfone	80
Appendix C Identification of NMR Spectrum of Polysulfone Sulfonated Polysulfone	83
Appendix D Thermogravimetric Analysis	85
Appendix E Proton Conductivity Under Dry State	89
Appendix F Proton Conductivity Under Wet State	109
Appendix G Methanol Permeability	127
Appendix H Water Uptake	150
Appendix I Mechanical Properties	154
Appendix J X-ray Photoelectron Spectroscopy (XPS)	165
Appendix K Scanning Electron Microscopy (SEM)	170
CURRICULUM VITAE	171

LIST OF TABLES

TABLE		PAGE
2.1	Proton conductivity and methanol permeability of PSF compared with Nafion in previous work	22
4.1	Proton conductivity and methanol permeability of S-PSF and composite membranes in the wet state at room temperature	67
4.2	Mechanical properties of S-PSF and composite membranes at 27 °C	68
A1	Sulfonation condition of PSF at 25 °C for 4 h for film casting	79
B1	The FT-IR absorption spectra of PSF and S-PSF	81
C1	Chemical Shift (ppm) from ¹ H-NMR spectra for S-PSF	84
D1	Thermal stability of S-PSF and S-PSF/Zeolite Y composite membranes	87
D2	Thermal stability of S-PSF/S-GO composite membranes	88
E1	Proton conductivity of the S-PSF/Zeolite Y composite membrane with a DS of 0.72 at 27 °C under dry state	96
E2	Proton conductivity of the S-PSF/S-GO composite membrane with a DS of 0.72 at 27 °C under dry state	104
E3	Proton conductivity of the hybrid membranes with a DS of 0.72 at 27 °C under dry state	108
F1	Proton conductivity of the S-PSF/Zeolite Y composite membrane at 27 °C under wet state	116
F2	Proton conductivity of the S-PSF/S-GO composite membrane with a DS of 0.72 at 27 °C under dry state	123
F3	Proton conductivity of the hybrid membranes with a DS of 0.72 at 27 °C under wet state	127
G1	Retention time composites	129
G2	Calibration concentration of methanol	130

TABLE	PAGE
G3 Methanol concentration in chamber A and B at 70 °C of S-PSF (DS 71.55%) and Nafion 117	137
G4 Methanol concentration in chamber A and B at 70 °C of S-PSF/Zeolite 5 % v/v composite membrane	137
G5 Methanol concentration in chamber A and B at 70 °C of S-PSF/10 %v/v Zeolite Y composite membrane	138
G6 Methanol concentration in chamber A and B at 70 °C of S-PSF/15 %v/v Zeolite Y composite membrane	139
G7 Methanol concentration in chamber A and B at 70 °C of S-PSF/20 %v/v Zeolite Y composite membrane	140
G8 Methanol concentration in chamber A and B at 70 °C of S-PSF/S-GO 1% v/v composite membrane	141
G9 Methanol concentration in chamber A and B at 70 °C of S-PSF/S-GO 2% v/v composite membrane	142
G10 Methanol concentration in chamber A and B at 70 °C of S-PSF/S-GO 3% v/v composite membrane	143
G11 Methanol concentration in chamber A and B at 70 °C of S-PSF/S-GO 5% v/v composite membrane	144
G12 Methanol concentration in chamber A and B at 70 °C of S-PSF/S-GO 7% v/v composite membrane	145
G13 Methanol permeability (cm ² /s) of S-PSF and S-PSF/Zeolite Y composite membranes	146
G14 Methanol permeability (cm ² /s) of S-PSF/S-GO composite membranes	147
G15 Methanol concentration in chamber A and B at 70 °C of S-PSF/3% v/v S-GO/12% v/v Zeolite Y composite membrane	148

TABLE	PAGE
G16 Methanol concentration in chamber A and B at 70 °C of S-PSF/3% v/v S-GO/15% v/v Zeolite Y composite membrane	149
G17 Methanol permeability (cm ² /s) of the hybrid membranes	150
H1 Water uptake of S-PSF and S-PSF/Zeolite Y composite membranes at 27 °C	152
H2 Water uptake of S-PSF/S-GO composite membranes at 27 °C	153
H3 Water uptake of the hybrid membranes at 27 °C	154
I1 Mechanical property of PSF	155
I2 Mechanical property of SPSF with DS of 0.72	155
I3 Mechanical property of S-PSF/5%v/v Zeolite Y composite membranes	156
I4 Mechanical property of S-PSF/10%v/v Zeolite Y composite membranes	156
I5 Mechanical property of S-PSF/15%v/v Zeolite Y composite membranes	156
I6 Mechanical property of S-PSF/20%v/v Zeolite Y composite membranes	157
I7 Mechanical property of S-PSF/5%v/v Zeolite Y composite membranes	158
I8 Mechanical property of S-PSF/1%v/v S-GO composite membranes	160
I9 Mechanical property of S-PSF/2%v/v S-GO composite membranes	160
I10 Mechanical property of S-PSF/3%v/v S-GO composite membranes	160
I11 Mechanical property of S-PSF/5%v/v S-GO composite membranes	161

TABLE		PAGE
I12	Mechanical property of S-PSF/5%v/v S-GO composite membranes	161
I13	Mechanical properties of S-PSF and S-PSF/S-GO composite membranes	162
I14	Mechanical property of S-PSF/ S-PSF/3%v/v S-GO and 12%v/v zeolite Y composite membranes	164
I15	Mechanical property of S-PSF/ S-PSF/3%v/v S-GO and 15%v/v zeolite Y composite membranes	164
I16	Mechanical properties of S-PSF and hybrid composite membranes	165
J1	Summary of S 2p and C 1s XPS spectral data	170

LIST OF FIGURES

FIGURE	PAGE
1.1	Schematic representation of a DMFC single cell. 2
2.1	Nafion's molecular structure, which is a copolymer of a Teflon backbone and sulfonyl groups. 6
2.2	Structure of polysulfone (PSF). 12
2.3	Structure of graphene oxide (GO). 31
4.1	FT-IR spectra of PSF and S-PSF with 0.72 of DS. 59
4.2	¹ H-NMR spectrum for S-PSF. 59
4.3	TGA thermograms of PSF and S-PSF with 0.72 of DS. 60
4.4	FTIR spectra of GO and S-GO. 60
4.5	Wide region XPS spectra of: (a) GO, (b) S-GO, (c) S2p spectra of GO, (d) S2p spectra of S-GO, (e) C1s spectra of GO and (f) C1s spectra of S-GO. 61
4.6	SEM images of the surface of: (a) GO and (b) S-GO. 62
4.7	TGA thermograms for S-PSF/Zeolite Y composite membranes. 62
4.8	TGA thermograms for S-PSF/S-GO composite membranes. 63
4.9	Water uptake (%) for S-PSF and S-PSF/Zeolite Y composite membranes. 63
4.10	Water uptake (%) for S-PSF and S-PSF/S-GO composite membranes. 64
4.11	Proton conductivity of the S-PSF/Zeolite Y composite membrane with a DS of 0.72 at 27 °C. 64

FIGURE	PAGE
4.12 Proton conductivity of the S-PSF/S-GO composite membrane with a DS of 0.72 at 27 °C.	65
4.13 Methanol permeability at 70 °C of S-PSF and S-PSF/Zeolite Y composite membranes.	65
4.14 Methanol permeability at 70 °C of S-PSF and S-PSF/S-GO composite membranes.	66
B1 FT-IR spectra of polysulfone (PSF) and sulfonated polysulfone (S-PSF) at 0.72 of degree of sulfonation.	80
C1 ¹ H-NMR spectrum for sulfonated Polysulfone (S-PSF).	83
C2 Chemical structure of Sulfonated Polysulfone (S-PSF).	84
D1 TGA thermograms of polysulfone (PSF) and sulfonated polysulfone (S-PSF) at 0.72 of degrees of sulfonation.	85
D2 TGA curve for S-PSF/Zeolite Y composite membranes.	86
D3 TGA curve for S-PSF/S-GO composite membranes.	86
E1 Nyquist plot of the Nafion117 membrane.	89
E2 Enlarged Nyquist plot of the Nafion117 membrane (R = 5.00 ohm).	90
E3 Nyquist plot of the S-PSF with a DS of 0.72 at 27 °C under dry state.	90
E4 Enlarged Nyquist plot of the S-PSF with a DS of 0.72 at 27 °C under dry state (R = 3.94 ohm).	91
E5 Nyquist plot of the S-PSF with 5% v/v of Zeolite Y at 27 °C under dry state.	91
E6 Enlarged Nyquist plot of the S-PSF with 5% v/v of Zeolite Y at 27 °C under dry state (R = 2.89 ohm).	92
E7 Nyquist plot of the S-PSF with 10% v/v of Zeolite Y at 27 °C under dry state.	92

FIGURE	PAGE
E8 Enlarged Nyquist plot of the S-PSF with 10% v/v of Zeolite Y at 27 °C under dry state (R = 1.05 ohm).	93
E9 Nyquist plot of the S-PSF with 15% v/v of Zeolite Y at 27 °C under dry state.	93
E10 Enlarged Nyquist plot of the S-PSF with 15% v/v of Zeolite Y at 27 °C under dry state (R = 0.96 ohm).	94
E11 Nyquist plot of the S-PSF with 20% v/v of Zeolite Y at 27 °C under dry state.	94
E12 Enlarged Nyquist plot of the S-PSF with 20% v/v of Zeolite Y at 27 °C under dry state (R = 1.41 ohm).	95
E13 Impedance of the S-PSF/Zeolite Y composite membrane with a DS of 0.72 at 27 °C under dry state.	96
E14 Proton conductivity of the S-PSF/Zeolite Y composite membrane with a DS of 0.72 at 27 °C under dry state.	97
E15 Nyquist plot of the S-PSF with 1% v/v of S-GO at 27 °C under dry state.	97
E16 Enlarged Nyquist plot of the S-PSF with 1% v/v of S-GO at 27 °C under dry state (R = 1.18 ohm).	98
E17 Nyquist plot of the S-PSF with 2% v/v of S-GO at 27 °C under dry state.	98
E18 Enlarged Nyquist plot of the S-PSF with 2% v/v of S-GO at 27 °C under dry state (R = 0.68 ohm).	99
E19 Nyquist plot of the S-PSF with 3% v/v of S-GO at 27 °C under dry state.	99
E20 Enlarged Nyquist plot of the S-PSF with 3% v/v of S-GO at 27 °C under dry state (R = 0.57 ohm).	100
E21 Nyquist plot of the S-PSF with 5% v/v of S-GO at 27 °C under dry state.	100

FIGURE	PAGE
E22 Enlarged Nyquist plot of the S-PSF with 5% v/v of S-GO at 27 °C under dry state (R = 1.18 ohm).	101
E23 Nyquist plot of the S-PSF with 7% v/v of S-GO at 27 °C under dry state.	101
E24 Enlarged Nyquist plot of the S-PSF with 7% v/v of S-GO at 27 °C under dry state (R = 1.31 ohm).	102
E25 Nyquist plot of the pristine S-GO at 27 °C under dry state.	102
E26 Enlarged Nyquist plot of the pristine S-GO at 27 °C under dry state.	103
E27 Impedance of the S-PSF/S-GO composite membrane with a DS of 0.72 at 27 °C under dry state.	105
E28 Proton conductivity of the S-PSF/S-GO composite membrane with a DS of 0.72 at 27 °C under dry state.	105
E29 Nyquist plot of the S-PSF with 3% v/v of S-GO and 12% v/v of zeolite Y at 27 °C under dry state.	106
E30 Enlarged Nyquist plot of the S-PSF with 3% v/v of S-GO and 12% v/v of zeolite Y at 27 °C under dry state (R = 0.61 ohm).	106
E31 Nyquist plot of the S-PSF with 3% v/v of S-GO and 15% v/v of zeolite Y at 27 °C under dry state.	107
E32 Enlarged Nyquist plot of the S-PSF with 3% v/v of S-GO and 15% v/v of zeolite Y at 27 °C under dry state (R = 0.77 ohm).	107
F1 Nyquist plot of the Nafion117 membrane.	109
F2 Enlarged Nyquist plot of the Nafion117 membrane (R = 0.18 ohm).	110
F3 Nyquist plot of the S-PSF with a DS of 0.72 at 27 °C under wet state.	110

FIGURE	PAGE
F4 Enlarged Nyquist plot of the S-PSF with a DS of 0.72 at 27 °C under wet state (R = 3.28 ohm).	111
F5 Nyquist plot of the S-PSF with 5% v/v of Zeolite Y at 27 °C under wet state.	111
F6 Enlarged Nyquist plot of the S-PSF with 5% v/v of Zeolite Y at 27 °C under wet state (R = 1.82 ohm).	112
F7 Nyquist plot of the S-PSF with 10% v/v of Zeolite Y at 27 °C under wet state.	112
F8 Enlarged Nyquist plot of the S-PSF with 10% v/v of Zeolite Y at 27 °C under wet state (R = 0.85 ohm).	113
F9 Nyquist plot of the S-PSF with 15% v/v of Zeolite Y at 27 °C under wet state.	113
F10 Enlarged Nyquist plot of the S-PSF with 15% v/v of Zeolite Y at 27 °C under wet state (R = 0.70 ohm).	114
F11 Nyquist plot of the S-PSF with 20% v/v of Zeolite Y at 27 °C under wet state.	114
F12 Enlarged Nyquist plot of the S-PSF with 20% v/v of Zeolite Y at 27 °C under wet state (R = 1.11 ohm).	115
F13 Impedance of the S-PSF/Zeolite Y composite membrane with a DS of 0.72 at 27 °C under wet state.	116
F14 Proton conductivity of the S-PSF/Zeolite Y composite membrane with a DS of 0.72 at 27 °C under wet state.	117
F15 Nyquist plot of the S-PSF with 1% v/v of S-GO at 27 °C under wet state.	117
F16 Enlarged Nyquist plot of the S-PSF with 1% v/v of S-GO at 27 °C under wet state (R = 0.98 ohm).	118
F17 Nyquist plot of the S-PSF with 2% v/v of S-GO at 27 °C under wet state.	118

FIGURE	PAGE
F18 Enlarged Nyquist plot of the S-PSF with 2% v/v of S-GO at 27 °C under wet state (R = 0.59 ohm).	119
F19 Nyquist plot of the S-PSF with 3% v/v of S-GO at 27 °C under wet state.	119
F20 Enlarged Nyquist plot of the S-PSF with 3% v/v of S-GO at 27 °C under wet state (R = 0.40 ohm).	120
F21 Nyquist plot of the S-PSF with 5% v/v of S-GO at 27 °C under wet state.	120
F22 Enlarged Nyquist plot of the S-PSF with 5% v/v of S-GO at 27 °C under wet state (R = 0.83 ohm).	121
F23 Nyquist plot of the S-PSF with 7% v/v of S-GO at 27 °C under wet state.	121
F24 Enlarged Nyquist plot of the S-PSF with 7% v/v of S-GO at 27 °C under wet state (R = 0.94 ohm).	122
F25 Impedance of the S-PSF/S-GO composite membrane with a DS of 0.72 at 27 °C under wet state.	124
F26 Proton conductivity of the S-PSF/S-GO composite membrane with a DS of 0.72 at 27 °C under wet state.	124
F27 Enlarged Nyquist plot of the S-PSF with 3% v/v of S-GO and 12% v/v of zeolite Y at 27 °C under wet state (R = 0.41 ohm).	125
F28 Enlarged Nyquist plot of the S-PSF with 3% v/v of S-GO and 12% v/v of zeolite Y at 27 °C under wet state (R = 0.41 ohm).	125
F29 Nyquist plot of the S-PSF with 3% v/v of S-GO and 15% v/v of zeolite Y at 27 °C under wet state.	126

FIGURE		PAGE
F30	Enlarged Nyquist plot of the S-PSF with 3% v/v of S-GO and 15% v/v of zeolite Y at 27 °C under wet state ($R = 0.53$ ohm).	126
G1	Calibration curve of methanol concentration versus the ratio of methanol and ethanol.	131
G2	Methanol concentration in chamber B versus time at 70°C of Nafion 117.	131
G3	Methanol concentration in chamber B versus time at 70 °C of S-PSF at DS 71.55%.	132
G4	Methanol concentration in chamber B versus time at 70 °C of S-PSF/Zeolite Y 5 % v/v.	132
G5	Methanol concentration in chamber B versus time at 70 °C of S-PSF/Zeolite Y 10 % v/v.	133
G6	Methanol concentration in chamber B versus time at 70 °C of S-PSF/Zeolite Y 15 % v/v.	133
G7	Methanol concentration in chamber B versus time at 70 °C of S-PSF/Zeolite Y 20 % v/v.	134
G8	Methanol concentration in chamber B versus time at 70 °C of S-PSF/S-GO 1 % v/v.	134
G9	Methanol concentration in chamber B versus time at 70 °C of S-PSF/S-GO 2 % v/v.	135
G10	Methanol concentration in chamber B versus time at 70 °C of S-PSF/S-GO 3 % v/v.	135
G11	Methanol concentration in chamber B versus time at 70 °C of S-PSF/S-GO 5 % v/v.	136
G12	Methanol concentration in chamber B versus time at 70 °C of S-PSF/S-GO 7 % v/v.	136

FIGURE	PAGE
G13 Methanol permeability at 70 °C of S-PSF and S-PSF/Zeolite Y composite membranes.	146
G14 Methanol permeability (cm ² /s) of S-PSF/S-GO composite membranes.	147
G15 Methanol concentration in chamber B versus time at 70 °C of S-PSF/3% v/v S-GO/12% v/v Zeolite Y.	148
G16 Methanol concentration in chamber B versus time at 70 °C of S-PSF/3% v/v S-GO/12% v/v Zeolite Y.	149
H1 Water uptake (%) for S-PSF and S-PSF/Zeolite Y composite membranes.	151
H2 Water uptake (%) for S-PSF and S-PSF/S-GO composite membranes.	154
I1 Tensile strength of S-PSF/zeolite Y composite membranes.	158
I2 Yield strain of S-PSF/zeolite Y composite membranes.	158
I3 Young's modulus of S-PSF/zeolite Y composite membranes.	159
I4 Tensile strength of S-PSF/S-GO composite membranes.	162
I5 Yield strain of S-PSF/S-GO composite membranes.	163
I6 Young's modulus of S-PSF/S-GO composite membranes.	163
J1 Wide region XPS spectra of GO.	166
J2 Wide region XPS spectra of S-GO.	167
J3 S2p region XPS spectra of GO.	167
J4 S2p region XPS spectra of S-GO.	168
J5 C1s region XPS spectra of GO.	168
J6 C1s region XPS spectra of S-GO.	169
K1 SEM images of the surface of: (a) GO and (b) S-GO.	171